Astronomy & Astrophysics

LETTER TO THE EDITOR

Herschel/SPIRE observations of the dusty disk of NGC 4244[⋆]

B. W. Holwerda[1], S. Bianchi[2], T. Böker[1], D. Radburn-Smith[4], R. S. de Jong[3], M. Baes[5], P. C. van der Kruit[6], M. Xilouris[7], K. D. Gordon[8], and J. J. Dalcanton[4]

[1] European Space Agency Research Fellow (ESTEC), Keplerlaan 1, 2200 AG Noordwijk, The Netherlands
   e-mail: benne.holwerda@esa.int
[2] INAF – Arcetri Astrophysical Observatory, Largo Enrico Fermi 5, 50125 Florence, Italy
[3] Department of Astronomy, University of Washington, Box 351580, Seattle, WA 98195, USA
[4] Leibniz Institut für Astrophysik Potsdam (AIP), An der Sternwarte 16, 14482 Potsdam, Germany
[5] Sterrenkundig Observatorium, Universiteit Gent, Krijgslaan 281-S9, 9000 Gent, Belgium
[6] Kapteyn Astronomical Institute, University of Groningen, PO Box 800, 9700 AV Groningen, The Netherlands
[7] Institute of Astronomy and Astrophysics, National Observatory of Athens, P. Penteli, 15236 Athens, Greece
[8] Space Telescope Science Institute, 3700 San Martin Drive, MD 21218, Baltimore, USA

ABSTRACT

We present *Herschel*/SPIRE images at 250, 350, and 500 μm of NGC 4244, a typical low-mass, disk-only and edge-on spiral galaxy. The dust disk is clumpy and shows signs of truncation at the break radius of the stellar disk. This disk coincides with the densest part of the H$\scriptstyle\rm I$ disk. We compare the spectral energy distribution (SED), including the new SPIRE fluxes, to 3D radiative transfer models; a smooth model disk and a clumpy model with embedded heating. Each model requires a very high value for the dust scale-length ($h_d = 2-5\,h_*$), higher dust masses than previous models of NGC 4244 ($M_d = 0.47-1.39 \times 10^7\ M_\odot$) and a face-on optical depth of $\tau_V^{\rm f.o.} = 0.4-1.12$, in agreement with previous disk opacity studies. The vertical scales of stars and dust are similar. The clumpy model much better mimics the general morphology in the sub-mm images and the general SED. The inferred gas-to-dust mass ratio is compatible with those of similar low-mass disks. The relatively large radial scale-length of the dust disk points to radial mixing of the dusty ISM within the stellar disk. The large vertical dust scale and the clumpy dust distribution of our SED model are both consistent with a scenario in which the vertical structure of the ISM is dictated by the balance of turbulence and self-gravity.

Key words. radiative transfer – dust, extinction – ISM: structure – galaxies: ISM – galaxies: spiral – galaxies: structure

1. Introduction

The edge-on perspective of a spiral galaxy's disk reveals both the vertical structure of the disk and its faint outskirts, thanks to line-of-sight integration. One typical feature is the mid-plane dust absorption lane. Dust is linked to the cold molecular ISM, mechanically (Allen et al. 1986; Weingartner & Draine 2001), through mutual shielding, and as a catalyst for molecular gas formation. Dalcanton et al. (2004) used the appearance of dust lanes as a probe of vertical stability of spiral disks. They found that in massive spirals, the ISM collapses into a thin dust-lane, while in low-mass disks ($v_{\rm rot} < 120$ km s^{-1}) the dust morphology is flocculant.

One comprehensive approach to investigate this phenomenon is to model the multi-wavelength information on a range of spiral disks with a spectral energy distribution (SED) model. Dust absorption, especially within the thin dark dust lane, is strongest at optical and ultra-violet wavelengths and the challenge for the models is to balance the observed absorption with the dust emission at far-infrared (FIR) and sub-millimeter (mm) wavelengths (e.g., Popescu et al. 2000; Misselt et al. 2001; Gordon et al. 2001; Alton et al. 2004; Bianchi 2008; Baes et al. 2010; Bianchi & Xilouris 2011). Until recently, these models were degenerate in the vertical distributions of stellar light and

ISM due to a lack of resolution and wavelength coverage in the FIR and sub-mm, but with the advent of the *Herschel* Space Observatory, the vertical structure of nearby edge-on disks can now be fully resolved.

Massive edge-on spiral galaxies have been observed by several *Herschel* surveys (see Boselli et al. 2010; Eales et al. 2010b; Davies et al. 2010) and a dedicated program[1] (Verstappen et al. in prep.) which targets seven massive spirals. Our NHEMESES[2] program aims to observe a complementary sample of low-mass nearby edge-ons. The combined observations will serve as a test for the different radiative transfer models in the literature; those from Baes et al. (2003, 2011), Bianchi (2007, 2008), Gordon et al. (2001), Misselt et al. (2001) and Pierini et al. (2004), and Popescu et al. (2000, 2011). These models will further test the suggested dichotomy in the vertical dust structure.

Here, we explore the first NHEMESES results on NGC 4244, the prototypical low-mass ($v_{\rm rot} = 95$ km s^{-1}), late-type (Sc), edge-on spiral at a distance[3] of 4.4 Mpc to compare to the first *Herschel* results on the massive edge-on spiral NGC 891 (Bianchi & Xilouris 2011). Originally, van der Kruit & Searle (1981) found a single edge-on exponential disk truncated at 9 kpc, later confirmed by Fry et al. (1999). The truncation

---

[1] HERschel Observations of Edge-on Spirals, HEROES.
[2] New HErschel Multi-wavelength Extragalactic Survey of Edge-on Spirals (Holwerda et al. 2011).
[3] The mean of the distances in NED from Heald et al. (2011b). Radburn-Smith et al. (2011) derive a distance of 4.7 Mpc.
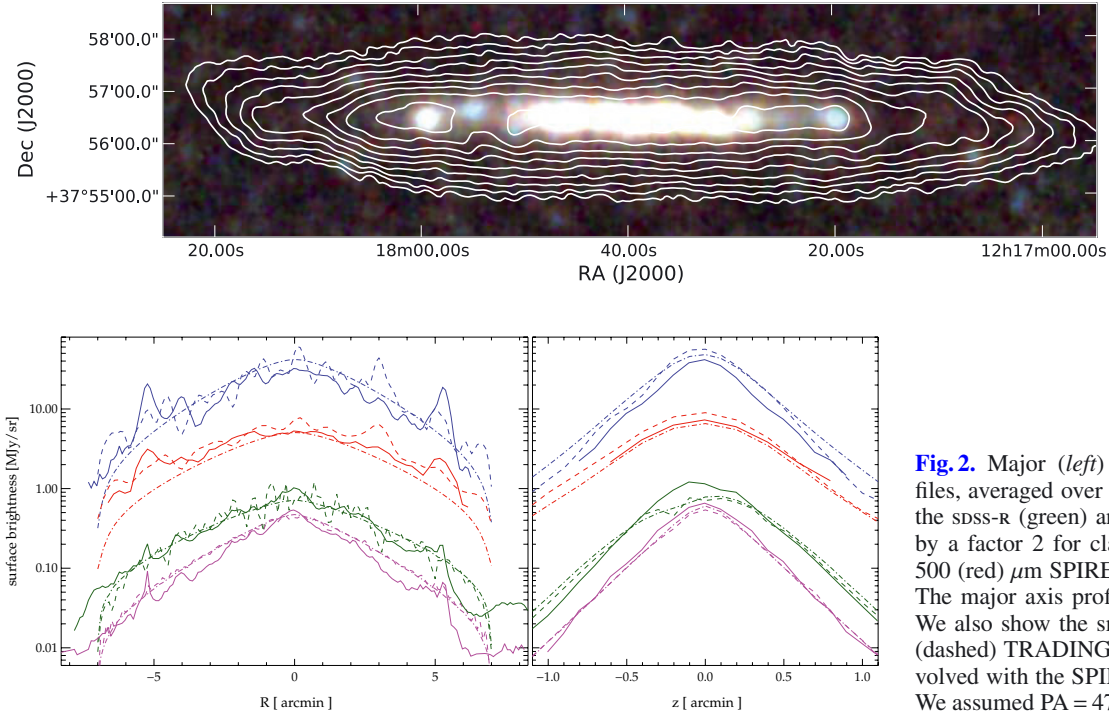
Fig. 1. A color composite of the SPIRE maps of NGC 4244, 250 (red), 350 (green), and 500 μm (blue) with the H I contours from Zschaechner et al. (2011) (contours at 6.4×10^{19} cm^{-2} increasing by factors of 2. The SPIRE flux stays within the 8.1×10^{19} cm^{-2} contour (second to highest).

Fig. 2. Major (*left*) and minor (*right*) axis profiles, averaged over a strip of 30″ (solid lines), in the sdss-r (green) and IRAC 3.6 μm (pink, offset by a factor 2 for clarity) and the 250 (blue) and 500 (red) μm SPIRE data, all at native resolution. The major axis profile spans $D_{25} = 16.6$ (RC3). We also show the smooth (dot-dash) and clumpy (dashed) TRADING models for comparison (convolved with the SPIRE PSFs at 250 and 500 μm). We assumed PA = 47.3° (de Jong et al. 2007).

was also observed with the *Hubble* Space Telescope (de Jong et al. 2007). Yoachim & Dalcanton (2006) note a second, thick stellar disk as doubtful, but Comerón et al. (2011) report both a thin and thick disk of equal mass. Its center hosts a rotating nuclear star-cluster (Seth et al. 2008), and the disk is classified as "corrugated" (Florido et al. 1991).

NGC 4244's ISM is mostly in a thin disk, both the ionized gas (Hoopes et al. 1999) and warm dust, implying a low specific star-formation rate (Kodaira & Yamashita 1996). The H I disk shows a clear warp, kinematic evidence for a compact dark matter halo, and lagging extra-planar gas (Olling 1996; Zschaechner et al. 2011; Heald et al. 2011a). The H_2 mass, based on CO observations, is $1.4 \times 10^7 M_\odot$ (Matthews & Wood 2001).

A recent SED model by MacLachlan et al. (2011) finds that most (80%) of the FIR emission could arise from an optically thin disk with a similar scale-height for both dust and stars (as did Seth et al. 2005, based on stellar populations), a dust scale-length 1.8 times the stellar one and a dust mass of $2.38 \times 10^6 M_\odot$. They note their model diverges from the observed disk in the FIR and that the dust model is still uncertain without sub-mm observations.

In this Letter, we present new SPIRE sub-mm observations of NGC 4244, adding spatial information on the cold dust, and present two TRADING models to illustrate the role of ISM geometry on the observed overall SED and the sub-mm images.

2. Observations

SPIRE (Spectral and Photometric Imaging REceiver, Griffin et al. 2010) instrument at 250, 350 and 500 μm onboard the ESA *Herschel* Space Observatory (Pilbratt et al. 2010) observed NGC 4244 at 250, 350 and 500 μm in large map mode, over $25' \times 25'$ centered on the object with two cross-scans, using a 30″ s^{-1} scan rate. Data-reduction is as in Bianchi & Xilouris (2011); we generated maps with the naïve map-making procedure within HIPE (Ott 2010), with pixel sizes of 6″, 8″, 12″ at 250, 350 and 500 μm, respectively (about 1/3 of the measured FWHM: ≈18″, 25″ and 36″), resulting in uniform backgrounds

and sky rms noise of 1, 0.6 and 0.3 MJy sr^{-1} respectively, Fig. 1). A color correction half-way between that for a point- and extended-source was implemented with a color-correction in between the point- and extended-source (marginally resolved vertically), we derive integrated fluxes of 15.9, 9.8, and 5.1 Jy (250, 350 and 500 μm), and adopt a conservative 15% calibration error.

3. Results and analysis

Figure 1 shows a SPIRE color-composite, together with the H I contours from Zschaechner et al. (2011). The dust emission falls entirely within the second highest H I contour, concentrated in a flat, single disk with no emission in the extended warped H I disk and envelope, in contrast to the more massive NGC 891, where Popescu & Tuffs (2003) and Bianchi & Xilouris (2011) find evidence for dust throughout the H I disk and the extended envelope (Oosterloo et al. 2007). Dust is concentrated in the thin H I disk, but we note that dust and H I clumps do not coincide.

Figure 2 shows the radial and vertical profiles of the sub-mm data, sdss-r data (Aihara et al. 2011), and the *Spitzer* 3.6 μm image from a related *Spitzer* program[4]. The sub-mm flux is contained within the D_{25} radius, and the profile shows clumps of emission at both ends of the disk. These clumps of sub-mm emission are the last reliable detection of the disk before the truncation radius (420″, 9 kpc van der Kruit & Searle 1981). The vertical sub-mm profiles are similar in width to those in *Spitzer* 3.6 μm emission, a good tracer of the stellar mass (e.g. Meidt et al. 2012). Figure 2 suggest that dust is confined to the thin disk, in contrast to NGC 891, where a second vertical component is observed (Kamphuis et al. 2007; Bianchi & Xilouris 2011), as well as a thin dust lane (Xilouris et al. 1999; Schechtman-Rook et al. 2012a,b).

Figure 3 shows the optical and infrared SED of the galaxy. The SPIRE flux densities show a spectral index $F_\nu \propto \nu^{1.6}$, flatter

---

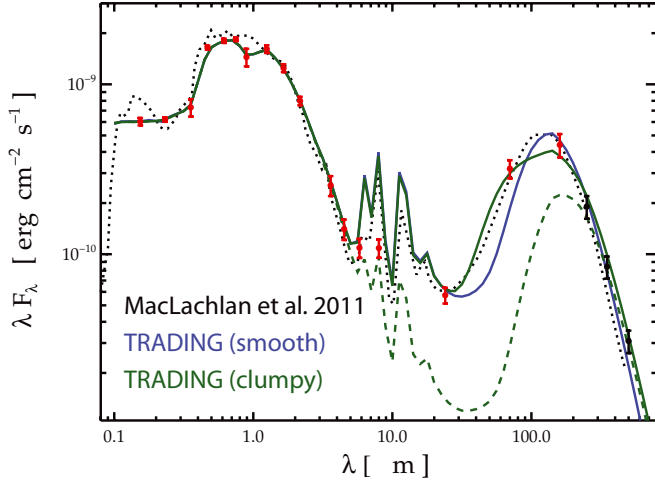[4] P.I. R. S. de Jong, Holwerda et al., in prep.

Fig. 3. The spectral energy distribution of NGC 4244. The *Herschel*/SPIRE fluxes from this work (black points) are show together with literature data (red symbols, Dale et al. 2009; MacLachlan et al. 2011). We show the smooth model (blue line); the clumpy model with and without embedded stellar emission (solid and dashed green line, respectively), and the model from MacLachlan et al. (black dotted line).

Table 1. Results from the SED models.

Parameter	MacLachlan et al. (2011)	Trading Smooth	Clumped	Unit
h_*	1.9	2.3	2.3	kpc
z_*, z_d	0.2	0.3	0.3	kpc
h_d	3.4	4.5 ($2h_*$)	9 = $r_{\rm trunc}$	kpc
$r_{\rm trunc}$	–	9	9	kpc
L_*	3.4×10^9	3.9×10^9	3.0×10^9	$L_\odot$
M_d	2.4×10^6	0.5×10^7	1.4×10^7	$M_\odot$
i	84.5°	88°	88°	
$L_{\rm cloud}$	1.0×10^8	–	3.7×10^8	$L_\odot$
$\tau_V^{\rm f.o.}$	0.2	0.4	1.1	
h_*/z_*	9.5	7.5	7.5	8.0 (3.6 μm)
h_d/z_d	17	15	30	10 (8.0 μm)

than the more massive NGC 891 ($F_\nu \propto \nu^{2.7}$), and thus indicative of a colder dust temperature (or of different dust properties). When compared to the radiative transfer model of MacLachlan et al. (2011), the observed fluxes at 350 and 500 μm are higher by a factor two (Fig. 3, Holwerda et al. 2011).

We model the surface brightness distribution and SED of NGC 4244 using the radiative transfer code TRADING (Bianchi 2008). We initialize the stellar distribution with the scale-length and height (h_*, z_*) as derived by Fry et al. (1999) (scaled to 4.4 Mpc), and adopted an intrinsic SED that, after being processed by dust, reproduces the observed stellar fluxes in the optical and NIR. We truncate the model, for both stars and dust, at 420″ (9 kpc) since it is to this radius we have reliable fluxes for both.

First, we try a *smooth* exponential dust disk with the same scale-height (z_d) as for stars, and modify the scale-length (h_d) and the central V-band face-on optical depth though the whole disk ($\tau_V^{\rm f.o.}$) to approximate both the sub-mm surface brightness profiles (Fig. 2) and the SED (Fig. 3). As MacLachlan et al. (2011), we require a dust scale-length larger than the stellar one to match the observed major axis profiles. However, contrary to MacLachlan et al. (2011), we need a higher opacity (and hence dust mass) to match the peak of the SED[5]. Ours and MacLachlan et al. (2011) models are compared in Table 1. While the smooth model can broadly match the peak of the SED and the profiles, it lacks hot dust to explain emission at 70 μm. And it underpredicts the 500 μm flux, implying a lower dust temperature[6].

Secondly, we consider an exclusively *clumpy* disk model; an exponential distribution of Giant Molecular Clouds (GMC), similar to the clumpy part of the smooth+clumpy model in Bianchi (2008) with $M_{\rm GMC} = 10^{6.5} M_\odot$, gas-to-dust mass ratio = 100, $R_{\rm GMC} \simeq 100$ pc. Bianchi (2008) find the SED does not depend

---

[5] Although the model of MacLachlan et al. (2011) includes a distribution of compact sources, with a dust mass about ten times than that of their diffuse disk, its contribution to the peak SED, as estimated from their Fig. 12, is smaller than 15%.

[6] Our assumption is that the dust grain population of NGC 4244 and Milky Way are identical but differences in sub-mm flux and optical extinction can be due to different grain distributions as well.

critically on the GMC size distribution. This model matches the sub-mm SED well but fails in the FIR (Fig. 3, dashed line). To match the 70 μm emission, we heat 60% of the clouds internally with a hot young starcluster ($T = 35\,000$ K, $1.56 \times 10^6 L_\odot$, Fig. 3 solid green line), similar to the second dense dust disk with young stars introduced by Popescu et al. (2000) to reconcile FIR and sub-mm fluxes. We note that PAH fluxes (e.g., *Spitzer* 8 μm) are not yet reproduced by this model but this may be solved with a range of cloud sizes and heating source types in a future iteration. The resulting heated clumpy model requires a large dust scale-length, $h_d \sim r_{\rm trunc}$, an increase in total dust mass (three times the *smooth* model mass) and some 60% of the GMCs to be internally heated (equivalent to ~12% $L_{\rm bol}$ of the stellar disk).

The smooth and partially heated clumpy SED models illustrate how, in the case of a small disk as NGC 4244, high-resolution sub-mm data reveals a dust disk with more cold dust than a FIR-only model, which is distributed more in clumps and throughout the stellar disk (similar scale-length and height as the stellar disk). A complete fit of the SED (including future *Herschel*/PACS observations) will be presented in the context of our complete low-mass edge-on sample.

4. Discussion

Stacked observations in the *Herschel* H-ATLAS survey (Eales et al. 2010a) point to specific characteristics ($T_d \sim 15$ K, $M_d \sim 10^7 M_\odot$) for blue, low-mass spirals (~$10^9 M_\odot$ stellar mass Bourne et al. 2012). NGC 4244's stellar and HI mass are 6 and $2.5 \times 10^9 M_\odot$ (Strickland et al. 2004; Zschaechner et al. 2011). Compared to the H-ATLAS results, our SED dust mass is reasonable and the gas-to-dust ratio (535–170 for the smooth and clumped model respectively) is in line with those found for smaller spiral disks (Leroy et al. 2009).

The central optical depth of $\tau_V^{\rm f.o.} \sim 0.45-1.12$ is similar to the face-on optical depths in occulting galaxies (White et al. 2000; Holwerda et al. 2007b) or distant galaxy counts (Holwerda et al. 2005, 2007a,c). We therefore feel confident that our SED model accurately reflects the true dust mass of NGC 4244.

The scale-length of the dust in the SED models is consistently much larger to the stellar one; a factor 1.8 to 4.9, depending on the model. For NGC 891, a ratio of 1.5–2 is typically found (Xilouris et al. 1999; Popescu et al. 2000, 2011; Driver et al. 2007; Bianchi 2008; Bianchi & Xilouris 2011). Similarly, Holwerda et al. (2009) and Holwerda et al. (2012) report a clumpy, extended and flat dust profile in a similar mass face-on galaxy occulting a distant bright bulge (2MASX J00482185-2507365, near NGC 253). These flat radial profiles of dust suggest radial mixing of the ISM to a similar

level found in the stellar disks (de Jong et al. 2007; Roškar et al. 2008, Radburn-Smith et al. 2012).

We find a dust scale-height similar to the stellar one, as do MacLachlan et al. (2011). They attribute this to either the flattening of dust disks (Dalcanton et al. 2004) or a smaller stellar scale-height due to inefficient dynamical heating of the stellar disk in lower mass galaxies (Bizyaev & Kajsin 2004). To distinguish between these two scenarios, we compare the oblateness (h/z) of the stellar and dust disk (Table 1) to those in Fig. 2 in Dalcanton et al. (2004). We also include the oblateness of the 3.6 and 8.0 μm *Spitzer* observations (Holwerda et al., in prep.). We note that the value for z_* of 300 pc is the scale-height of the thin disk found by Comerón et al. (2011) and RGB stars (Seth et al. 2005). NGC 4244's stellar disk oblateness is at the highest, i.e., flattest value for low-mass disks, similar to the oblateness of massive disks, arguing against the less efficient disk heating compared to massive disks. The dusty disk oblateness is extremely high, even compared to the PAH emission ($h/z = 10$ at 8 μm), but this is predominantly because of the large scale-length of the dust disk. The similar stellar and dust scale-height and the best match by clumpy SED model are both consistent with the scenario from Dalcanton et al. (2004); in a low-mass disk such as this one, the ISM does not collapse into a thin plane but remains fractured and spread throughout the height of the stellar disk.

5. Summary and conclusions

Based on new sub-mm observations with the *Herschel* Space Observatory of NGC 4244, and some illustrative models with the TRADING code, we find that:

i.   The cold dust is confined to the inner, flat H I disk (Fig. 1).
ii. The dusty ISM is confined to the stellar radius (Fig. 2).
iii. A smooth model under-predicts 70 and 500 μm fluxes (Fig. 3).
iv. A clumpy dust disk model with a fraction of the clumps heated by embedded sources fits both the general SED (Fig. 3) and the morphology of the disk (Fig. 2) in sub-mm well.
vi. The inferred scales of stars and dust are consistent with a scenario that includes some radial migration of dust and a vertical ISM scale supported by turbulence (Table 1).

Future improvements of the NGC 4244 SED model includes new FIR (*Herschel*/PACS) information to constrain the cold dust structure and the number of GMCs and the stellar type of their heating sources. We plan to put these results in the context of the full NHEMESES and HEROES *Herschel* observations to infer if there is indeed a phase-change with mass in the dust structure and additionally to benchmark current SED models.

References

Aihara, H., Allende Prieto, C., An, D., et al. 2011, ApJS, 193, 29
Allen, R. J., Atherton, P. D., & Tilanus, R. P. J. 1986, Nature, 319, 296
Alton, P. B., Xilouris, E. M., Misiriotis, A., Dasyra, K. M., & Dumke, M. 2004, A&A, 425, 109
Baes, M., Davies, J. I., Dejonghe, H., et al. 2003, MNRAS, 343, 1081
Baes, M., Fritz, J., Gadotti, D. A., et al. 2010, A&A, 518, L39
Baes, M., Verstappen, J., De Looze, I., et al. 2011, ApJS, 196, 22
Bianchi, S. 2007, A&A, 471, 765
Bianchi, S. 2008, A&A, 490, 461
Bianchi, S., & Xilouris, E. M. 2011, A&A, 531, L11
Bizyaev, D., & Kajsin, S. 2004, ApJ, 613, 886
Boselli, A., Eales, S., Cortese, L., et al. 2010, PASP, 122, 261
Bourne, N., Maddox, S. J., Dunne, L., et al. 2012, MNRAS, 421, 3027
Comerón, S., Knapen, J. H., Sheth, K., et al. 2011, ApJ, 729, 18
Dalcanton, J. J., Yoachim, P., & Bernstein, R. A. 2004, ApJ, 608, 189
Dale, D. A., Cohen, S. A., Johnson, L. C., et al. 2009, ApJ, 703, 517
Davies, J. I., Baes, M., Bendo, G. J., et al. 2010, A&A, 518, L48
de Jong, R. S., Seth, A. C., Radburn-Smith, D. J., et al. 2007, ApJ, 667, L49
Driver, S. P., Popescu, C. C., Tuffs, R. J., et al. 2007, MNRAS, 563
Eales, S., Dunne, L., Clements, D., et al. 2010a, PASP, 122, 499
Eales, S. A., Smith, M. W. L., Wilson, C. D., et al. 2010b, A&A, 518, L62
Florido, E., Battaner, E., Sanchez-Saavedra, M. L., Prieto, M., & Mediavilla, E. 1991, MNRAS, 251, 193
Fry, A. M., Morrison, H. L., Harding, P., & Boroson, T. A. 1999, AJ, 118, 1209
Gordon, K. D., Misselt, K. A., Witt, A. N., & Clayton, G. C. 2001, ApJ, 551, 269
Griffin, M. J., Abergel, A., Abreu, A., et al. 2010, A&A, 518, L3
Heald, G., Allan, J., Zschaechner, L., et al. 2011a, IAU Symp. 277, in ed. C. Carignan, F. Combes, & K. C. Freeman, 59
Heald, G., Józsa, G., Serra, P., et al. 2011b, A&A, 526, A118
Holwerda, B. W., González, R. A., Allen, R. J., & van der Kruit, P. C. 2005, AJ, 129, 1396
Holwerda, B. W., Draine, B., Gordon, K. D., et al. 2007a, AJ, 134, 2226
Holwerda, B. W., Keel, W. C., & Bolton, A. 2007b, AJ, 134, 2385
Holwerda, B. W., Meyer, M., Regan, M., et al. 2007c, AJ, 134, 1655
Holwerda, B. W., Keel, W. C., Williams, B., Dalcanton, J. J., & de Jong, R. S. 2009, AJ, 137, 3000
Holwerda, B. W., Bianchi, S., Baes, M., et al. 2011 [arXiv:1109.5603]
Holwerda, B. W., Dalcanton, J. J., Keel, W. C., Boeker, T., & de Jong, R. S. 2012, MNRAS, submitted
Hoopes, C. G., Walterbos, R. A. M., & Rand, R. J. 1999, ApJ, 522, 669
Kamphuis, P., Holwerda, B. W., Allen, R. J., Peletier, R. F., & van der Kruit, P. C. 2007, A&A, 471, L1
Kodaira, K., & Yamashita, T. 1996, PASJ, 48, 581
Leroy, A. K., Walter, F., Bigiel, F., et al. 2009, AJ, 137, 4670
MacLachlan, J. M., Matthews, L. D., Wood, K., & Gallagher, J. S. 2011, ApJ, 741, 6
Matthews, L. D., & Wood, K. 2001, ApJ, 548, 150
Meidt, S. E., Schinnerer, E., Knapen, J. H., et al. 2012, ApJ, 744, 17
Misselt, K. A., Gordon, K. D., Clayton, G. C., & Wolff, M. J. 2001, ApJ, 551, 277
Olling, R. P. 1996, AJ, 112, 457
Oosterloo, T., Fraternali, F., & Sancisi, R. 2007, AJ, 134, 1019
Ott, S. 2010, in Astronomical Data Analysis Software and Systems XIX, ed. Y. Mizumoto, K.-I. Morita, & M. Ohishi, ASP Conf. Ser., 434, 139
Pierini, D., Gordon, K. D., Witt, A. N., & Madsen, G. J. 2004, ApJ, 617, 1022
Pilbratt, G. L., Riedinger, J. R., Passvogel, T., et al. 2010, A&A, 518, L1
Popescu, C. C., & Tuffs, R. J. 2003, A&A, 410, L21
Popescu, C. C., Misiriotis, A., Kylafis, N. D., Tuffs, R. J., & Fischera, J. 2000, A&A, 362, 138
Popescu, C. C., Tuffs, R. J., Dopita, M. A., et al. 2011, A&A, 527, A109
Radburn-Smith, D. J., de Jong, R. S., Seth, A. C., et al. 2011, ApJS, 195, 18
Radburn-Smith, D. J., Röskar, R., Dalcanton, J. J., et al. 2012, ApJ, accepted
Roškar, R., Debattista, V. P., Stinson, G. S., et al. 2008, ApJ, 675, L65
Schechtman-Rook, A., Bershady, M. A., & Wood, K. 2012a, ApJ, 746, 70
Schechtman-Rook, A., Bershady, M. A., Wood, K., & Robitaille, T. P. 2012b [arXiv:1203.0023]
Seth, A. C., Dalcanton, J. J., & de Jong, R. S. 2005, AJ, 129, 1331
Seth, A., Agüeros, M., Lee, D., & Basu-Zych, A. 2008, ApJ, 678, 116
Strickland, D. K., Heckman, T. M., Colbert, E. J. M., Hoopes, C. G., & Weaver, K. A. 2004, ApJS, 151, 193
van der Kruit, P. C., & Searle, L. 1981, A&A, 95, 105
Weingartner, J. C., & Draine, B. T. 2001, ApJ, 553, 581
White, III, R. E., Keel, W. C., & Conselice, C. J. 2000, ApJ, 542, 761
Xilouris, E. M., Byun, Y. I., Kylafis, N. D., Paleologou, E. V., & Papamastorakis, J. 1999, A&A, 344, 868
Yoachim, P., & Dalcanton, J. J. 2006, AJ, 131, 226
Zschaechner, L. K., Rand, R. J., Heald, G. H., Gentile, G., & Kamphuis, P. 2011, ApJ, 740, 35